RESEARCH PAPERS

An effective absorbing boundary algorithm for acoustical wave propagator*

Lin Zhibin**, Lu Jing and Xu Boling

(Key Laboratory of Modern Acoustics, Institute of Acoustics, Nanjing University, Nanjing 210093, China)

Accepted on February 9, 2007

Abstract In this paper, Berenger's perfectly matched layer (PML) absorbing boundary condition for electromagnetic waves is introduced as the truncation area of the computational domain to absorb one-dimensional acoustic wave for the scheme of acoustical wave propagator (AWP). To guarantee the efficiency of the AWP algorithm, a regulated propagator matrix is derived in the PML medium. Numerical simulations of a Gaussian wave packet propagating in one-dimensional duct are carried out to illustrate the efficiency of the combination of PML and AWP. Compared with the traditional smoothing truncation windows technique of AWP, this scheme shows high computational accuracy in absorbing acoustic wave when the acoustical wave arrives at the computational edges. Optimal coefficients of the PML configurations are also discussed.

Keywords: acoustical wave propagator; perfectly matched layer; absorbing boundary conditions (ABC).

Recently, the acoustical wave propagator scheme which investigates the propagation and scattering of acoustic waves has been developed[1] and extended by many researchers[2—5]. This technique involves an effective time-domain calculation of sound propagation using the combination of Chebyshev polynomial and the Fourier pseudo-spectral method, which allows effective and accurate prediction of wave packet evolution with large time steps. However, as a method of numerically simulating acoustic wave propagation, artificial boundaries must be introduced into the AWP (acoustical wave propagator) to limit the area of computation. To eliminate the spurious reflections produced by these artificial boundaries, absorbing boundary conditions are needed. The traditional approach of the AWP uses the technique of smoothing truncation windows to smooth the outer-going waves at the boundary, which is not optimal enough for higher computational accuracy. The computational edges should be properly considered for the AWP.

The perfectly matched layer is currently a popular absorbing boundary condition for numerical modeling of electromagnetic, acoustic and elastic wave problems, which was first introduced by Berenger for electromagnetic waves[6—8]. It is based on the use of an absorbing layer especially designed to absorb without reflection the electromagnetic waves. In that approach, a PML (perfectly matched layer) medium of a certain depth is introduced in a region adjacent to the artificial boundary of a computational domain. After careful design of the parameter, the impedance of the PML, as proved by Berenger[6], is the same as that of the interior lossless medium and then the interface between the physical domain and the absorbing layer does not produce spurious reflections inside the domain of interest. Consequently, the PML provides an ideal ABC for the truncation of the computational domain in numerical methods such as the finite-difference, finite-element, and pseudo-spectral time-domain methods[9—12].

In this paper, the AWP algorithm in conjunction with the PML technique (PML-AWP) is considered for one-dimensional case studies of acoustical wave propagation. The proper general AWP matrix is derived in the PML medium and the optimal parameter of the PML is also discussed. Simulation results verify that the proposed method leads to more accurate computational result than that of the traditional

* Supported by National Natural Science Foundation of China (Grant Nos. 60340420325 and 10604030) and the Research Fund for the Doctoral Program of Higher Education of China (Grant No. 20040284038)

** To whom correspondence should be addressed. E-mail: linzhibin@nju.org.cn

smoothing truncation windows of original AWP, especially in the vicinity of the computational boundaries. In this paper, we combine the AWP algorithm with the PML technique and derive a regulated propagator matrix. Several illustrating examples are presented to illustrate the efficiency of the PML-AWP.

1 Some theories of the acoustical wave propagator

1.1 Theory and implementation of acoustical wave propagator[1]

The technique of AWP is based on the coupled first-order linear acoustic propagation equations

$$\begin{cases} \rho \dfrac{\partial v(x,t)}{\partial t} = -\nabla p(x,t) \\ \dfrac{1}{\rho c^2} \dfrac{\partial p(x,t)}{\partial t} = -\nabla v(x,t) \end{cases} \tag{1}$$

where $v(x,t)$ represents the acoustic particle velocity, $p(x,t)$ is the acoustic pressure fluctuation, ρ is the density of the medium, and c is the sound speed.

On the other hand, the linear acoustical wave equation mentioned above can be described by

$$\frac{\partial}{\partial t}\Phi(x,t) = -\boldsymbol{H}\Phi(x,t) \tag{2}$$

where x denotes the spatial coordinates, $\Phi(x,t)$ is the state vector, and $\boldsymbol{H}$ is a spatial derivative operator. For one-dimensional acoustical wave equation, $\Phi(x,t)$ can be represented as the sound pressure $p(x,t)$ and the particle velocity $v(x,t)$

$$\Phi(x,t) = \begin{bmatrix} p(x,t) \\ v(x,t) \end{bmatrix} \tag{3}$$

Then

$$\boldsymbol{H} = \begin{bmatrix} 0 & \rho c^2 \dfrac{\partial}{\partial x} \\ \dfrac{1}{\rho}\dfrac{\partial}{\partial x} & 0 \end{bmatrix} \tag{4}$$

Integrating Eq. (2) with respect to time, we can obtain

$$\Phi(x,t) = \mathrm{e}^{-(t-t_0)\boldsymbol{H}}\Phi(x,t_0) \tag{5}$$

In this way, the state vector at any time t can be evaluated by the operation of the acoustical wave propagator $\mathrm{e}^{-(t-t_0)\boldsymbol{H}}$ acting upon the initial state vector $\Phi(x,t_0)$. The characteristics of the media can be included in the AWP matrix $\boldsymbol{H}$.

For the convenience of the calculation, the AWP matrix needs to be normalized by[2]

$$\boldsymbol{H}' = \frac{\boldsymbol{H}}{|\lambda|_{\max}} \tag{6}$$

where $|\lambda|_{\max}$ is the maximum eigen-value of the AWP matrix. Denote $R = (t-t_0)|\lambda|_{\max}$, then the acoustical wave propagator can be expanded by Chebyshev polynomials of the first kind as

$$\mathrm{e}^{-(t-t_0)\boldsymbol{H}} = \mathrm{e}^{-R\boldsymbol{H}'} = \sum_{n=0}^{\infty} a_n(R)T_n(\boldsymbol{H}') \tag{7}$$

where $a_n(R) = 2J_n(R)$ except for $a_0(R) = J_0(R)$ and $J_n(R)$ is the nth-order Bessel function of the first kind. The zero- and first-order Chebyshev polynomials are defined as $T_0(\boldsymbol{H}') = \boldsymbol{I}$ and $T_1(\boldsymbol{H}') = \boldsymbol{H}'$, and the rest can be calculated by the following recursive relations

$$T_{n+1}(\boldsymbol{H}') = 2\boldsymbol{H}'T_n(\boldsymbol{H}') + T_{n-1}(\boldsymbol{H}') \tag{8}$$

Eq. (5) then becomes

$$\Phi(x,t) = \mathrm{e}^{-(t-t_0)\boldsymbol{H}}\Phi(x,t_0) = \sum_{n=0}^{\infty} a_n(R)T_n(\boldsymbol{H}')\Phi(x,t_0) \tag{9}$$

The spatial derivatives within the AWP matrix $\boldsymbol{H}$ are calculated by the spectral method as

$$\frac{\partial^n}{\partial x^n}\psi(x,t) = F^{-1}\{(jk)^n F[\psi(x,t)]\} \tag{10}$$

where $F[\,]$ and $F^{-1}[\,]$ represent the Fourier transform and the inverse Fourier transform, respectively, and k is the wave number.

The acoustical wave propagator combines the spectral method in frequency-domain with the Chebyshev polynomial expansion in time-domain. As a result, it is a highly efficient calculation technique for calculating the time-domain evolution of the acoustical wave[1-5].

1.2 Gaussian smoothing truncation windows in the AWP

In the original AWP, the truncation of the computational domain is simulated by introducing a Gaussian truncation function in the vicinity of the computational edges. In one-dimensional case, the computational domain is set as $[x_1, x_2]$ and $x_2 - x_1 = L$. For an N-gird-point Fourier pseudo-spectral method used in AWP, in order to minimize reflections from the truncated boundary, a truncated window of length m is implemented at the edges of $x = x_1$ and $x = x_2$ as

$$Wd(n\cdot\Delta) = \begin{cases} 0 & n = 0, 1, \cdots, m-1 \text{ and} \\ & n = N-m, N-m+1, \cdots, \\ & N-1 \\ 1 & n = m, m+1, \cdots, N-m-1 \end{cases} \tag{11}$$

where Δ is the spatial sample interval. To remove the

discontinuity at $x=(m-1)\cdot\Delta$ and $x=(N-m)\cdot\Delta$, a Gaussian function $G(x)$ is applied to convolve with the window function $Wd(n\cdot\Delta)$ as[1]

$$\widehat{Wd}(x)=F^{-1}\{F[Wd(x)]F[e^{-(\xi-x)^2/b^2}]\} \tag{12}$$

where $x=n\cdot\Delta$ and b controls the effective width of the Gaussian function.

In the original AWP, the Gaussian truncation windows mentioned above are used as the absorbing boundary to absorb the outgoing wave when it arrives at the computational edges. However, the truncation window length should be large enough to guarantee the calculation precision, which leads to a heavy computational burden. Furthermore, for higher dimensional AWP, the reflection of the computational edge becomes increasingly obvious and the simple truncation windows cannot absorb the out-going waves effectively.

2 Acoustical wave propagator in a PML medium

2.1 PML technique for the acoustical wave propagator

The perfectly matched layer is realized from the physical absorption of the incident numerical wave by means of a lossy medium. This is devised using a novel split-field formulation of Maxwell's equations where each vector field component is split into two or three orthogonal components[6—8]. The novelty of this technique lies in the way through which the layer equations are constructed. However, for one-dimensional acoustical wave, only one component exists in the layer equations. Thus, for all real acoustical media and for the purposes of equation symmetry of the original PML form, we only need to introduce two damping coefficients, and correspondingly the first order acoustic equations in a one-dimensional homogeneous medium should be[9, 12]

$$\begin{cases}\nabla p(x,t)=-\rho\dfrac{\partial}{\partial t}\boldsymbol{v}(x,t)-\alpha^{*}\boldsymbol{v}(x,t)\\ \nabla\cdot\boldsymbol{v}(x,t)=-\dfrac{1}{\rho c^2}\dfrac{\partial}{\partial t}p(x,t)-\alpha p(x,t)\end{cases} \tag{13}$$

where $\boldsymbol{v}(x,t)$ is the acoustic particle velocity, $p(x,t)$ is the acoustic pressure fluctuation, ρ is the density of the medium, and c is the sound speed of the medium. Two attenuation coefficients α^{*} and α are introduced as damping terms. As a result, they are included here since the PML method relies on the introduction of nonphysical density attenuation in the absorbing layers. To implement the PML in the technique of AWP, Eq. (13) can be reformed as

$$\begin{cases}\dfrac{\partial}{\partial t}p(x,t)=-\rho c^2\alpha p(x,t)-\rho c^2\cdot\nabla\cdot\boldsymbol{v}(x,t)\\ \dfrac{\partial}{\partial t}\boldsymbol{v}(x,t)=-\dfrac{1}{\rho}\nabla p(x,t)-\dfrac{\alpha^{*}}{\rho}\boldsymbol{v}(x,t)\end{cases} \tag{14}$$

For one-dimensional case, define a state vector for sound field $\Phi=\begin{bmatrix}p(x,t)\\ v(x,t)\end{bmatrix}$, then Eq. (14) can be simplified as

$$\frac{\partial\Phi}{\partial t}=-\boldsymbol{H}\Phi \tag{15}$$

where

$$\boldsymbol{H}=\begin{bmatrix}\rho c^2\alpha & \rho c^2\nabla\\ \dfrac{1}{\rho}\nabla & \dfrac{\alpha^{*}}{\rho}\end{bmatrix} \tag{16}$$

Eq. (15) indicates the acoustical wave propagator equations for the sound field in a PML medium, whose operation matrix is $\boldsymbol{H}$. The theory of PML[9] indicates that if

$$\rho c^2\alpha=\frac{\alpha^{*}}{\rho} \tag{17}$$

then the lossy PML medium causes unreflective transmission of acoustical wave propagating normally across the interface between the lossless acoustical medium (with $\alpha^{*}=\alpha=0$) and the PML medium (with $\rho c^2\alpha=\dfrac{\alpha^{*}}{\rho}\neq 0$).

Substituting Eq. (17) into Eq. (16), the AWP matrix becomes

$$\boldsymbol{H}=\begin{bmatrix}\delta & \rho c^2\nabla\\ \dfrac{1}{\rho}\nabla & \delta\end{bmatrix} \tag{18}$$

where $\delta=\rho c^2\alpha=\dfrac{\alpha^{*}}{\rho}$. Eq. (18) indicates that the regulated AWP in the PML medium and the original AWP in the lossless medium can be unified in terms of the change of the damping coefficients in one-dimensional case. It should be noted here that the extension of the scheme to two-dimensional case and three-dimensional case will be straightforward. For example, for two-dimensional calculation, following Berenger[6], the pressure and velocity can be expanded as $p=p_x+p_y$ and $v=v_x+v_y$, and the attenuation parameters δ_x and δ_y are introduced to rewrite the PML pressure-velocity Eq. (14). It should be noted here that, while v_x and v_y are the physical

components of velocity, p_x, p_y and δ_x, δ_y have no physical meanings. Following the similar deduction process as the one-dimensional case, the state vector for two-dimensional sound field is

$$\Phi = \begin{bmatrix} p_x(x, y, t) \\ p_y(x, y, t) \\ v_x(x, y, t) \\ v_y(x, y, t) \end{bmatrix} \tag{19}$$

Then the AWP matrix becomes

$$\boldsymbol{H} = \begin{bmatrix} \delta_x & 0 & \rho c^2 \frac{\partial}{\partial x} & 0 \\ 0 & \delta_y & 0 & \rho c^2 \frac{\partial}{\partial y} \\ \frac{1}{\rho}\frac{\partial}{\partial x} & \frac{1}{\rho}\frac{\partial}{\partial x} & \delta_x & 0 \\ \frac{1}{\rho}\frac{\partial}{\partial y} & \frac{1}{\rho}\frac{\partial}{\partial y} & 0 & \delta_y \end{bmatrix} \tag{20}$$

It can be seen from Eqs. (19) and (20) that the implementation of two-dimensional PML-AWP will be the same as that of one-dimensional case. However, the split forms of pressure and velocity make the AWP matrix lose its symmetry, which results in some difficulties of the calculation. In addition, the split version of the PML equations admits instability waves which, if not suppressed by numerical dissipation or other means, could ruin the numerical solution[13]. Detailed analysis of the higher-dimensional AWP combined with a PML medium is ongoing and will be addressed in the following paper.

2.2 Implementation of the PML boundary for the acoustical wave propagator

The PML technique assumes a certain thickness of an artificial absorbing medium at the two ends of one-dimensional duct. As shown in Fig. 1, the computational domain with an interior region and the PML boundary regions is constructed by defining the PML with w samples length.

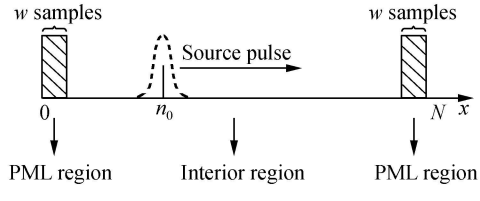

Fig. 1. Geometry of the AWP grid with the PML boundary regions.

For the left and right ends of the PML regions, δ increases from zero to δ_{max} smoothly from the inner to the outer boundary. For the left end region in Fig. 1,

$$\delta(i) = \delta_{max} \cdot \left| \frac{w - i}{w} \right|^{\gamma}, \quad i = 0, \cdots, w - 1 \tag{21}$$

and for the right end region in Fig. 1,

$$\delta(i) = \delta_{max} \cdot \left| \frac{N - w - i}{w} \right|^{\gamma}, \quad i = N - w, \cdots, N - 1 \tag{22}$$

where w and N are the length of the PML layers and the number of the AWP grid, respectively, δ_{max} is the maximum damping coefficient at the outer boundary and γ is the order of the polynomial grading. However, for the interior region, to simulate a lossless acoustic medium, the damping coefficient is set to zero as

$$\delta(i) = 0, \quad i = w, w + 1, \cdots, N - w \tag{23}$$

It should be noted here that δ_{max} is determined by the reduction of acoustical wave propagation at a distance of Δ, which will be discussed and optimized in the following section.

3 Simulation results

In this section, several illustrating examples for the combination of AWP with PML are presented. The one-dimensional acoustic wave propagation is initialized by a Gaussian wave packet as

$$p(x, 0) = e^{-\frac{(x - x_0)^2}{a^2}} \tag{24}$$

$$v(x, 0) = \frac{1}{\rho c} e^{-\frac{(x - x_0)^2}{a^2}} \tag{25}$$

where x_0 is the initial position of the incident Gaussian wave packet and a is the width coefficient of this packet. In the following simulations, the computational domain of length 20 m is chosen which is located in [0 m, 20 m]. The density of air is $\rho = 1.21$ kg/m^3 and the velocity of sound is $c = 344$ m/s. The initial Gaussian wave packet is centered at the position of $x_0 = 15$ m and the number of the total grid points is $N = 1024$. The maximum damping coefficient δ_{max} will be selected after some computational efforts of estimating global error.

For the conveniences of the discussion, a global normalized error function over the computational domain is defined as

$$\text{Error}(T) = 10\log 10 \left[\frac{\int_{x_1}^{x_2} |p_{re}(x, T)|^2 dx}{\int_{x_1}^{x_2} |p_0(x, 0)|^2 dx} \right] \tag{26}$$

where T is the total transmission time of Gaussian wave packet, $p_{re}(x, T)$ represents the spurious reflected wave in the computational domain caused by the computational boundary. $p_0(x, 0)$ denotes the initial Gaussian wave packet.

Fig. 2 compares the global errors derived from the proposed PML-AWP with that from the original AWP with smoothing truncated windows at different absorbing boundary points. The maximum damping coefficient ($\delta_{max}=0.8$) and the order of the polynomial grading ($\gamma=2$) are used in this simulation problem. As shown in Fig. 2, the advantage of the PML-AWP technique over original AWP with smoothing truncated windows is obvious. For the absorbing boundary layer with less than 11 points, the PML-AWP scheme achieves more than 20 dB decrease of the global normalized error.

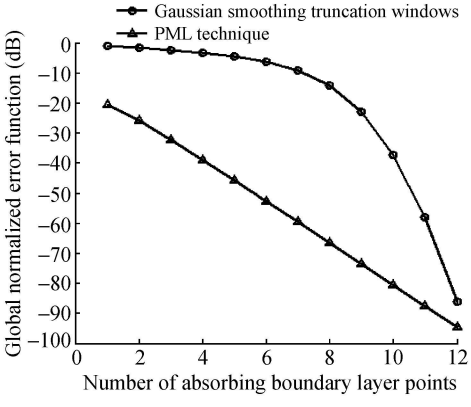

Fig. 2. Global normalized error of the proposed PML-AWP and the original AWP with smoothing truncated windows.

The following simulations are aimed to investigate the influence of the maximum damping coefficient δ_{max} and the order of the polynomial grading γ on the global error. The number of the PML points w equals 8.

It can be seen from Fig. 3 and Fig. 4 that proper configurations of the PML-AWP will greatly decrease the global error. If δ_{max} or γ is small, reflections from the PML external boundary will greatly influence the performance of the AWP algorithm, and the PML layers cannot provide satisfactory absorption of the transmitted wave. On the other hand, abrupt changes of the acoustical parameters are inevitable if δ_{max} or γ is too large, and the AWP algorithm will suffer from the error caused by Gibbs phenomenon[2]. In these simulations, we suggest $0.4\leqslant\delta_{max}\leqslant0.8$ and $1\leqslant\gamma\leqslant4$ for higher computational accuracy, minimum global error as well as numerical stability for the PML-AWP technique with eight-point boundary layer.

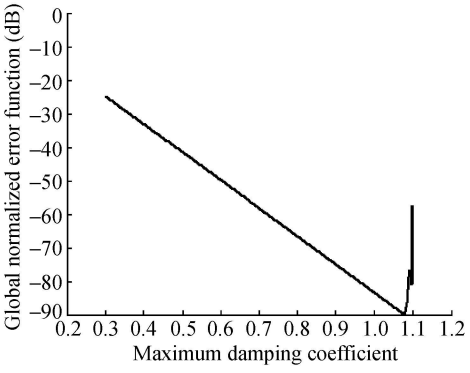

Fig. 3. Global normalized error versus the variation of the maximum damping coefficient.

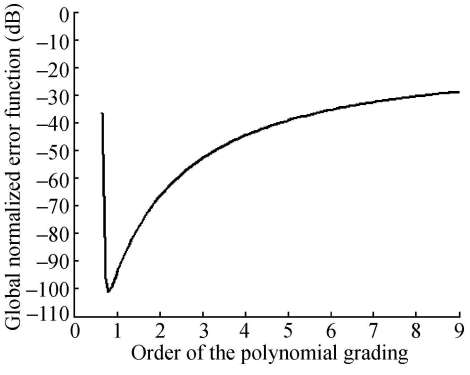

Fig. 4. Global normalized error versus the variation of the order of the polynomial grading.

4 Conclusions

In this paper, to reduce the spurious reflection caused by the computational boundary in the implementation of AWP, a regulated AWP matrix is deduced for the combination of PML with one-dimensional AWP. Several numerical simulations are carried out to verify the efficiency of the proposed scheme. The results demonstrate that, after proper selection of the parameters for the PML-AWP, higher computational accuracy is achieved and fewer points of the absorbing boundary are needed when comparing the original AWP with smoothing truncated windows. In addition, some efforts are also made to optimize the relevant parameters of the proposed scheme. However, difficulties remain in extending this scheme to two-dimensional and three-dimensional cases. Research aiming at dissolving these problems has been carried out.

References

1 Pan J and Wang JB. Acoustical wave propagator. Journal of the Acoustical Society of America, 2000, 108(2): 481—487

2 Lu J, Pan J and Xu BL. Time-domain calculation of acoustical wave propagation in discontinuous media using acoustical wave propagator with mapped pseudo-spectral method. Journal of the Acoustical Society of America, 2005, 118(6): 3408—3419

3 Peng SZ and Pan J. Acoustical wave propagator for time-domain dynamic stress concentration in a plate with a sharp change of section. Journal of the Acoustical Society of America, 2004, 117(2): 492—502

4 Peng SZ and Pan J. Acoustical wave propagator technique for time-domain reflection and transmission of flexural wave packets in one-dimensional stepped beams. Journal of Sound and Vibration, 2006, 297: 1025—1047

5 Wang JB and Pan J. Acoustical wave propagator with modified Chebyshev expansion. Computer Physics Communications, 2006, 174: 187—190

6 Berenger JP. A perfectly matched layer for the absorption of electro-magnetic wave. Journal of Computational Physics, 1994, 114: 185—200

7 Berenger JP. Perfectly matched layer for the FDTD solution of wave structure interaction problems. IEEE Transactions on Antennas and Propagation, 1996, 44: 110—117

8 Berenger JP. Three dimensional perfectly matched layer for the absorption of electromagnetic waves. Journal of Computational Physics, 1996, 114: 363—379

9 Yuan XJ, David B, James WW, et al. Formulation and validation of Berenger's PML absorbing boundary for the FDTD simulation of acoustic scattering. IEEE Transactions on Ultrasonics, Ferroelectrics and Frequency Control, 1997, 44(4): 816—822

10 Yuan XJ, David B, James WW, et al. Simulation of acoustic wave propagation in dispersive media with relaxation losses by using FDTD method with PML absorbing boundary condition. IEEE Transactions on Ultrasonics, Ferroelectrics and Frequency Control, 1999, 46(1): 14—23

11 Liu QH and Tao JP. The perfectly matched layer for acoustic waves in absorptive media. Journal of the Acoustical Society of America, 1997, 102(4): 2072—2082

12 Katsibas TK and Antonopoulos CS. A general form of perfectly matched layers for three-dimensional problems of acoustic scattering in lossless and lossy fluid media. IEEE Transactions on Ultrasonics, Ferroelectrics and Frequency Control, 2004, 51(8): 964—972

13 Hu FQ. On Absorbing Boundary Conditions for Linearized Euler Equations by a Perfectly Matched Layer. Journal of Computational Physics, 1996, 129: 201—219

Withdrawal

A multi-layer zone model for predicting temperature distribution in a fire room

CHEN Xiaojun, YANG Lizhong, DENG Zhihua, FAN Weicheng

2004, 14(6): 536—540

This manuscript is withdrawn from publication by the journal of *Progress in Natural Science* Editor-in-Chief. The basis for the withdrawal is a violation of the Ethical Guidelines of National Natural Science Foundation of China. Essentially the materials reported in this paper were plagiarized from K. A. Suzuki' work "Multi-layer zone model for predicting fire behavior in a single room", which was presented at the 7th International Symposium on Fire Safety Science in 2002. The corresponding author did not notice the deceitful behavior of the first author of this manuscript.